BJPS

Brazilian Journal of Pharmaceutical Sciences

DOI: http://dx.doi.org/10.1590/s2175-97902026e24378

Article

Activities, network pharmacology, potential mechanism against inflammation of a homogeneous polysaccharide MCP-1 from *Mesona chinensis Benth*

Chushan Chen[1], Haoming Chen[1], Juntao Xie[1], Yi Chen[1], Xin Yu[1], Hongxia Fan[1], Jiajin Huang[1], Huiqin Lu[2], Junxia Zheng[1*]**

[1]College of Biomedical and Pharmaceutical Sciences, Guangdong University of Technology, Guangzhou, Guangdong, China, [2]Guangdong Second Provincial General Hospital, Guangzhou, Guangdong, China

Inflammation is a condition in which the body's immune system is compromised. Polysaccharides from *Mesona chinensis* Benth have been shown to repair the immune system and inhibit inflammation. This study aimed to investigate the activities, network pharmacology, and potential mechanisms of action against inflammation of a homogeneous polysaccharide, MCP-1, from *M. chinensis.* MCP-1 was isolated and purified using water extraction, alcohol precipitation, the Sevag method, and column chromatography. The molecular weight of MCP-1 was determined to be 70.9kDa. The polysaccharide composition included glucose (39.05%), arabinose (18.31%), galactose (14.80%), galacturonic acid (13.98%), xylose (7.42%), mannose (4.14%), and glucuronic acid (2.30%). MCP-1 showed strong inhibitory effects on the release of NO, IL-6, and TNF-α (30.79±4.13%, 30.51±3.25%, and 37.25±3.57%, respectively). A total of 169 targets were identified based on the monosaccharide structures of MCP-1, with 9 targets associated with inflammation, including TLR4, STAT3, MMP9, COL18A1, TLR9, ABCB1, PPARA, MMP2, and NR1H4. The principal targets for anti-inflammatory therapies were associated with various signaling pathways involved in cancer and immune responses. Molecular docking experiments revealed that MCP-1 exhibited a high binding affinity for MMP2.

Keywords: *Mesona chinensis* Benth. Polysaccharide. Anti-inflammatory activity. Network pharmacology. Molecular docking.

INTRODUCTION

The active ingredients in Chinese herbal plants primarily include polyphenols, flavonoids, terpenes, alkaloids, and polysaccharides (Zheng *et al.*, 2019). Among these, polysaccharides are widely found in the roots, stems, and leaves of plants, with their content varying according to geographical and climatic factors (Zhang *et al.*, 2022). Due to their complex structures and diverse sources, natural polysaccharides have considerable potential for drug development, particularly in the area of anti-inflammatory drugs (Zhao *et al.*, 2020).

Mesona chinensis Benth, a plant belonging to the Lamiaceae family, is primarily distributed in regions such as Taiwan, Jiangxi, Guangdong, western Guangxi, Vietnam, and Myanmar (Lin *et al.*, 2017). It has been shown to possess significant anti-tumor, antioxidant, and hypoglycemic properties (Huang *et al.*, 2021). Recent studies on *M. chinensis* have identified its active ingredients, including flavonoids, phenylpropanoids, and polysaccharides.

Inflammation is a dynamic process involving injury, anti-injury, and repair. It includes three main stages: tissue damage, the production of inflammatory stress by inflammatory cells, and the repair of inflammatory tissues by white blood cells (Mack, 2018). With the accelerating pace of modern life, factors such as diet and lifestyle habits have increased the promotion of inflammatory processes, leading to the onset of inflammation (Mandelli *et al.*, 2023). Therefore, the search for safe and effective natural anti-inflammatory agents has become a major focus in anti-inflammatory drug research (Hou *et al.*, 2020).

***Correspondence:** J. Zheng, College of Biomedical and Pharmaceutical Sciences, Guangdong University of Technology, Guangzhou, Guangdong, 510006, P. R China, E-mail: junxiazheng@gdut.edu.cn, https://orcid.org/0000-0002-1107-6284 ** H. Lu, Guangdong Second Provincial General Hospital, Guangzhou, Guangdong, 510317, P. R China, E-mail: 178315573@qq.com, https://orcid.org/0000-0002-6446-6702

Polysaccharides in Chinese herbal medicine exhibit multi-level, multi-target characteristics, which align with the mechanisms of multi-target separation in network pharmacology (Zhao *et al.*, 2023). Establishing Compound-Target-Pathway interaction networks and comparing drug targets with those in databases provides a way to explore new drug targets and mechanisms (Liu *et al.*, 2024). Molecular docking serves as an effective tool for screening drug targets, enabling the exploration of potential disease targets within Chinese herbal polysaccharides.

In this study, a homogeneous polysaccharide, MCP-1, was isolated from *M. chinensis*, and its anti-inflammatory effects were evaluated using the Lipopolysaccharide (LPS)-induced RAW264.7 cell model to assess the release of Nitric Oxide (NO), Tumor Necrosis Factor-alpha (TNF-α), and Interleukin-6 (IL-6). Additionally, relevant inflammation-related targets of MCP-1 were identified, and molecular docking was performed to explore potential targets. This research lays the foundation for the development of novel anti-inflammatory pharmaceuticals.

MATERIAL AND METHODS

Material

M. chinensis was purchased from Rao Ping County, Chaozhou City, Guangdong Province, China. LPS and dextran standards (with molecular weights of 2.5 kDa, 11.6 kDa, 23.8 kDa, 48.6 kDa, 148 kDa, 273 kDa, 410 kDa, and 668 kDa) were obtained from Sigma-Aldrich Chemical Co. (St. Louis, MO, USA). Methylthiazolyldiphenyl-tetrazolium bromide (MTT) was purchased from Solarbio (Beijing, China). All reagents were of analytical grade and used before their expiration dates.

Preparation of polysaccharide

Figure 1A illustrates the extraction and purification process of the MCP-1 fraction from *M. chinensis*. Briefly, the water extract was first collected and deproteinized to produce crude polysaccharide MCP. This was then purified using DEAE-52 (2.3 × 70 cm) and Sephadex G-100 (1.8 × 100 cm) columns following decolorization, yielding the polysaccharide MCP-1. The polysaccharide content of MCP-1 was determined using the phenol-sulfuric acid method with glucose as a standard (DuBois *et al.*, 1956). Protein content was measured using the Bradford method with bovine serum albumin as the standard (Bradford, 1976).

Molecular weight detection

Gel permeation chromatography (E2695, Waters, USA) was used to determine the molecular weight of the polysaccharide. The dextran standards (2.5 kDa, 11.6 kDa, 23.8 kDa, 48.6 kDa, 148 kDa, 273 kDa, 410 kDa, 668 kDa) and MCP-1 were dissolved in the mobile phase (0.02 M $KHPO_4$) to form a 1 mg/mL solution. They (10 μL) were then eluted with the mobile phase into a refractive index detector (2414, Waters, USA) at a flow rate of 0.5 mL/min, using a TSK-GEL G-5000PWXL column (7.8 × 300 mm) and a TSK-GEL G-3000PWXL column (7.8 × 300 mm) in series. Dextran standards were used to generate a calibration curve for calculating the molecular weight of MCP-1 based on retention time.

Monosaccharide composition analysis

A standard solution of 10 mg/mL of 16 monosaccharide standards (Fuc, GalN, Rha, Ara, GlcN, Gal, Glc, GlcNAc, Xyl, Man, Fru, Rib, GalA, GulA, GlcA, ManA) was prepared. To analyze the monosaccharide composition, 10 mg of MCP-1 was hydrolyzed in 10 mL of 3 M TFA at 120°C for 3 hours. After hydrolysis, the solution was evaporated to dryness under a nitrogen stream, and 5 mL of water was added, followed by vortex mixing. The mixture was centrifuged at 12,000 rpm for 5 min, and the supernatant was analyzed by ion chromatography (ICS5000, ThermoFisher, USA). A 5 μL sample was eluted with a mobile phase comprising A: H2O, B: 15 mM NaOH, and C: 15 mM NaOH and 100 mM NaOAC

at 0.3 mL/min using a DionexCarbopac^{TM}PA20 column (3.0 × 150 mm) at 30°C. The elution gradient was as follows: 0 min Phase A/B/C (98.8:1.2:0, V/V), 18 min Phase A/B/C (98.8:1.2:0, V/V), 20 min Phase A/B/C (50:50:0, V/V), 30 min Phase A/B/C (50:50:0, V/V), 30.1 min Phase A/B/C (0:0:100, V/V), 46 min Phase A/B/C (0:0:100, V/V), 46.1 min Phase A/B/C (0:100:0, V/V), 50 min Phase A/B/C (0:100:0, V/V), 50.1 min Phase A/B/C (98.8:1.2:0, V/V), and 80 min Phase A/B/C (98.8:1.2:0, V/V).

UV analysis

A 5 mg polysaccharide sample was dissolved in deionized water to prepare a 2 mg/mL polysaccharide solution. The solution was scanned in the wavelength range of 200–800 nm using a UV-Vis spectrophotometer (TU-1901, Persee, China).

FT-IR analysis and Congo red test

FT-IR analysis of MCP-1 was performed as described in previous research (Luo *et al.*, 2022). A 3 mg polysaccharide sample was mixed with potassium bromide, pressed into small tablets, and scanned in the range of 500-4500cm^{-1} using an FT-IR spectrometer (iS50R, ThermoFisher, USA).

The Congo red test was conducted following the methodology reported with minor modifications to improve the process (Sun *et al.*, 2018). Briefly, 5 mg of MCP-1 was mixed with 2 mL of Congo red solution (concentration: 80 μmol/L) and 2 mL of distilled water. Various amounts of a 1.00 mol/L NaOH solution (ranging from 0 to 2.00 mL) were added to adjust the final NaOH concentration to 0–0.50 mol/L. A control group was prepared by mixing 2 mL of Congo red solution (80 μmol/L) with varying volumes of NaOH (1.00 mol/L) and distilled water. The maximum absorption wavelength ($\lambda_{\_max}$) was determined in the 200–800 nm range using a UV-Vis spectrophotometer (TU-1901, Persee, China).

Scanning electron microscope (SEM) and Atomic force microscope (AFM) analysis

Morphological characterization of MCP-1 was performed using a SEM (SU8220, Hitachi, Japan). The MCP-1 sample (5–10 mg/mL) was prepared, fixed, dehydrated, and coated with a thin metallic conductive layer. The surface image of the sample was obtained at magnifications of 500× and 2000×.

The surface topography of MCP-1 was assessed using an AFM (Dimension FastScan, Bruker, USA). A clean mica sheet was prepared and attached to MCP-1, which was then placed on the AFM stage for surface scanning. The resulting images were analyzed to measure parameters such as size, height, and distribution of MCP-1.

Cell culture and Cytotoxicity assay

RAW264.7 cells (obtained from the Shanghai Cell Bank, catalog number: SCSP-5036) were cultured in DMEM medium supplemented with 10% fetal bovine serum (FBS), 1% penicillin (100 μg/mL), and 1% streptomycin (100 μg/mL) at 37°C in a humidified atmosphere with 5% CO_2. Cytotoxicity of MCP-1 on RAW264.7 cells was evaluated using the MTT assay. Briefly, RAW264.7 cells were seeded in 96-well flat-bottomed plates at a density of 1×10^4 cells per well and cultured for 12 hours. The medium was replaced with MCP-1 dissolved in basal medium, diluted to concentrations ranging from 10 to 200 μg/mL, and incubated for 24 hours. After treatment, the medium was removed, and 50 μL of MTT solution (final concentration 5 mg/mL) was added to each well. After a 4-hour incubation, 150 μL of DMSO was added to dissolve the formazan crystals, and the absorbance at 570 nm (OD_{570nm}) was measured. The control group, which did not receive MCP-1 treatment, was used for comparison.

Detection of NO and TNF-α, IL-6 cytokines

RAW264.7 cells were pre-cultured in 24-well plates for 12 hours at a density of 1×10^6 cells per well. After 12 hours, the cell culture supernatant was collected, and the concentration of NO was determined using a commercial kit. Similarly, TNF-α and IL-6 levels were measured using ELISA kits. The blank control group, which did not receive MCP-1 or LPS treatment, was used for comparison.

Collection of potential targets against inflammation

Potential targets of MCP-1 monosaccharides were predicted based on their SMILES strings. Inflammation-related targets were retrieved from the GeneCards database. The PPI network was constructed using Cytoscape 3.10.1 software (https://cytoscape.org/), and Venn Diagrams was created to identify overlapping targets.

Go and KEGG enrichment analysis

Key targets were uploaded to the David database (https://david.ncifcrf.gov/) for Gene Ontology (GO) and Kyoto Encyclopedia of Genes and Genomes (KEGG) pathway enrichment analysis. GO analysis included three categories: biological process (BP), cellular component (CC), and molecular function (MF). KEGG analysis focused on inflammation-related pathways. GO and KEGG analysis figures were generated for visualization.

Molecular docking

Seven monosaccharide structures of MCP-1 were obtained in ".mol2" format. These structures were hydrogenated and saved as ".pdbqt" files. The target proteins were obtained from the PDB database, processed by dehydration and hydrogenation, and exported as pdbqt files using Pymol software (https://pymol.org/) to enable docking with monosaccharide molecules. Molecular docking was conducted using AutoDock Vina 4.1, Discovery Studio, Pymol 1.5.7 and Ligplot$^+$ software.

Statistical analysis

Statistical analysis was performed using GraphPad Prism version 8.4.3. Data are presented as mean ± standard deviation (SD). A p-value greater than 0.05 was considered non-significant. Analysis of variance (ANOVA) was used to evaluate significant differences between groups.

RESULTS

Isolation and purification of polysaccharides

The isolation and purification process of MCP-1 is depicted in Figure 1A. Briefly, the main polysaccharide fraction was obtained by purifying crude polysaccharides using a DEAE-52 column (Figure 1B), following deproteinization, decolorization, and precipitation with 95% ethanol at 4°C overnight. The primary fraction was then freeze-dried and further purified via a Sephadex G-100 column (Figure 1C), resulting in the purified MCP-1. The polysaccharide content of MCP-1 was 91.25 ± 1.36% ($y = 4.7954x + 0.0417$, $R^2 = 0.9994$), whereas the protein content was 1.94 ± 0.23% ($y = 0.0029x + 0.4405$, $R^2 = 0.9935$).

UV analysis of MCP-1

Figure 2A presents the UV absorption spectrum of MCP-1 in the range of 200–400 nm. No significant absorption peaks were observed in the 260–280 nm range, indicating minimal nucleic acid and protein content.

Molecular weight detection of MCP-1

The homogeneity of the purified polysaccharide was confirmed by a single, symmetrical elution peak in the GPC spectrum of MCP-1 (Figure 2B). Using a standard

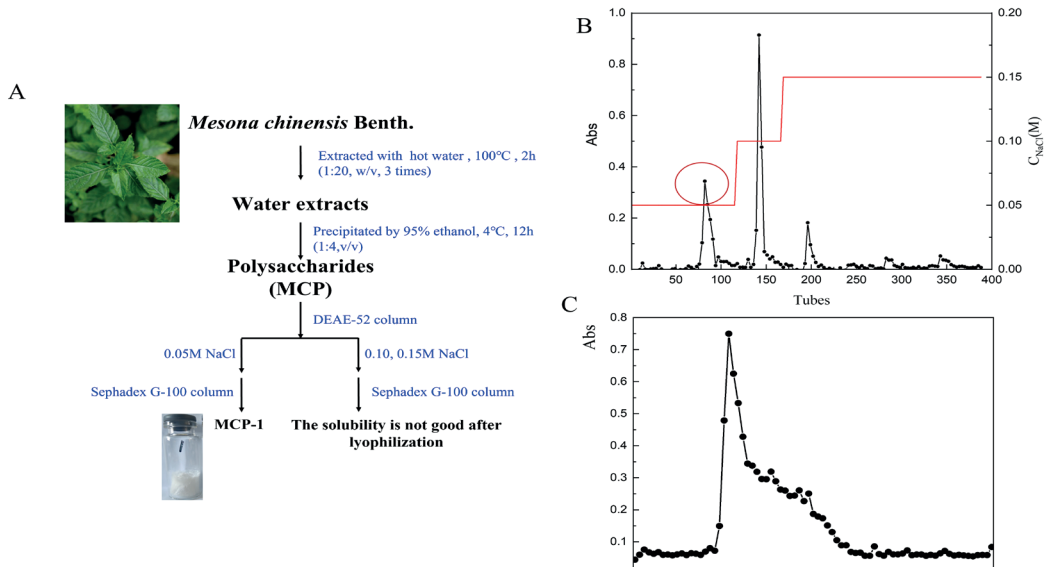

FIGURE 1 - The extraction and purification of MCP-1 (A); the purification of MCP-1 on DEAE-52 column (B); the purification of MCP-1 on Sephadex G-100 column (C).

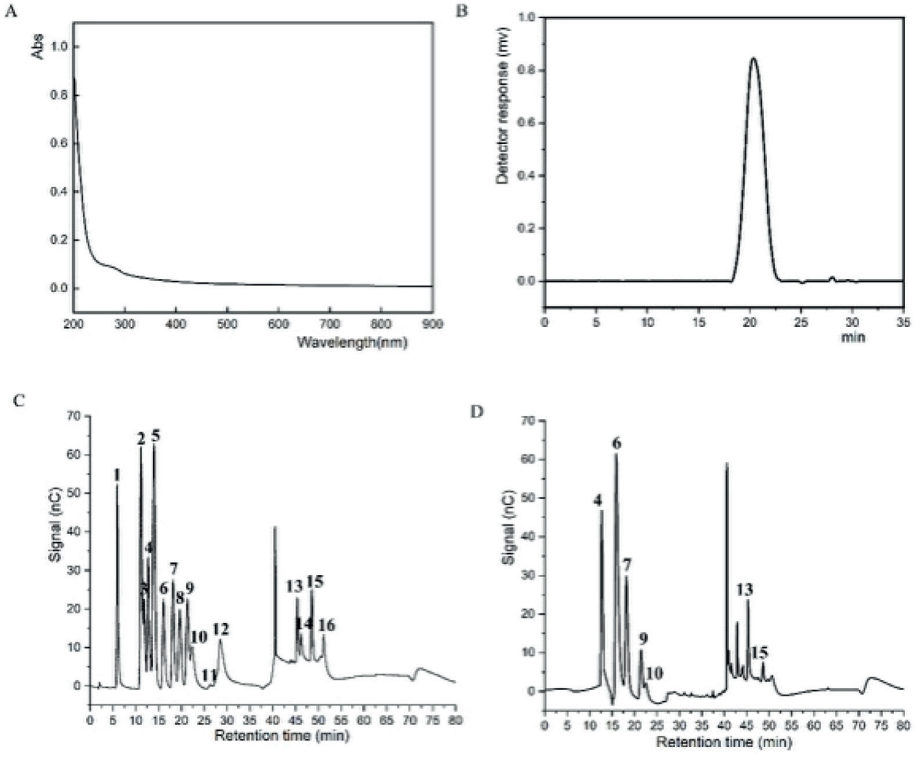

FIGURE 2 - UV spectra of MCP-1 (A); The molecular weight (Mw) distribution of MCP-1 (B); Monosaccharide composition analysis of standard substance, 1. Fuc, 2. GalN, 3. Rha, 4. Ara, 5. GlcN, 6. Gal, 7. Glc, 8.GlcNAc, 9. Xyl, 10. Man, 11.Fru, 12.Rib, 13.GalA, 14.GulA, 15.GlcA, 16 ManA(C); Monosaccharide composition analysis of MCP-1 (D).

calibration curve, the weight-average molecular weight of MCP-1 was calculated to be 70.9kDa (log M_W = −0.2582x + 10.141, R^2 = 0.9974).

Monosaccharide composition analysis of MCP-1

Figure 2C shows the standard sample diagram. As shown in Figure 2D, the monosaccharide composition of MCP-1 was found to consist of glucose (39.05%), arabinose (18.31%), galactose (14.80%), galacturonic acid (13.98%), xylose (7.42%), mannose (4.14%), and glucuronic acid (2.30%).

FT-IR analysis and Congo red test of MCP-1

The FT-IR spectrum of MCP-1 (Figure 3A) revealed peaks at 3439 cm^{-1} (O-H stretching), 2926 cm^{-1} (C-H stretching), 1639 cm^{-1} (C=O antisymmetric stretching), 1386 cm^{-1} (C-H bending), and 1022 cm^{-1} (pyran ring stretching). The absorption peak at 895 cm^{-1} confirmed the presence of a β-glycosidic bond. Peaks at 871 cm^{-1} and 811 cm^{-1} indicated the presence of mannose (Hoseiniyan Benvidi and Jahanbin, 2020).

As shown in Figure 3B, the maximum wavelength of the Congo red signal shifted in the presence of NaOH concentrations ranging from 0.0 M to 0.1 M, suggesting the formation of a complex between Congo red and MCP-1, and the formation of a triple-helix structure. As the NaOH concentration increased, the triple-helix conformation of MCP-1 was disrupted, resulting in an asymmetric coil structure. These results suggest that MCP-1 adopts a well-organized helical shape in slightly alkaline conditions (Guo *et al.*, 2021).

SEM images analysis and AFM images analysis

SEM analysis, an important tool for examining the structure and activity of materials, revealed the surface topography of MCP-1 at magnifications of 500× and 2000×. The images showed the presence of thick flakes, substantial aggregates, and elongated structures (Figure 4A). After hot water extraction, the structural integrity of the polysaccharides was compromised, displaying numerous fine pores, consistent with findings from previous studies (Li *et al.*, 2012).

AFM analysis was employed to measure the surface height of MCP-1. As shown in Figure 4B, the surface morphology of MCP-1 consisted of curved and stubby chains, with particle and block heights of 327.3 nm and 389.8 nm, respectively.

The effect of MCP-1 on the viability of RAW264.7 cells

The cytotoxicity of MCP-1 on RAW264.7 cells was

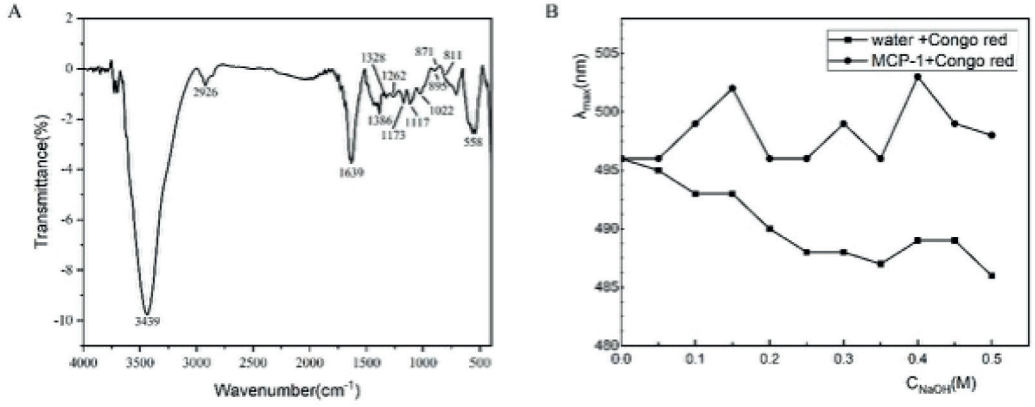

FIGURE 3 - FI-IR analysis of MCP-1 (A); Congo red test of MCP-1 (B).

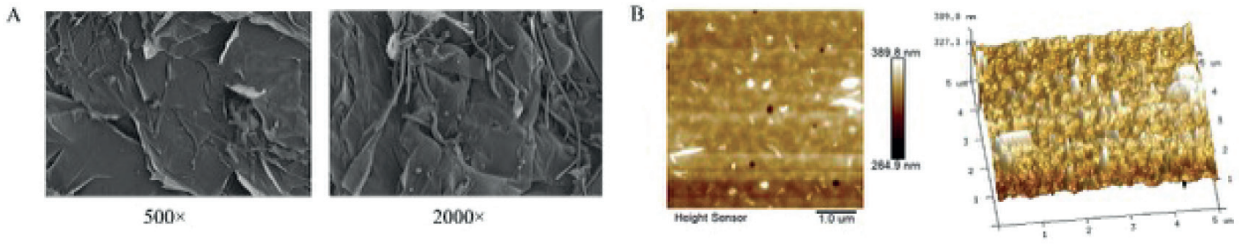

FIGURE 4 - SEM spectra of MCP-1 (500× and 2000 ×): MCP-1 (A) and AFM 2D & 3D images (B).

assessed using the MTT assay at concentrations ranging from 25 to 800 μg/mL. As shown in Figure 5A, exposure to low concentrations of MCP-1 (25–100 μg/mL) did not result in a statistically significant reduction in cell viability compared to the control group, suggesting that low concentrations of MCP-1 do not adversely affect the viability of RAW264.7 cells ($P > 0.05$). However, at higher concentrations (200–800 μg/mL), MCP-1 significantly reduced cell viability, suggesting that higher concentrations of MCP-1 inhibit the migration and proliferation of RAW264.7 cells, whereas lower concentrations have negligible effects.

The effect of MCP-1 on LPS-induced inflammatory

The anti-inflammatory properties of MCP-1 were evaluated using the LPS-induced RAW264.7 cell model. Compared to the control group, LPS stimulation significantly increased the production of NO, TNF-α, and IL-6 ($p < 0.001$). Pretreatment with MCP-1 significantly inhibited the release of NO and TNF-α (30.79 ± 4.13% and 37.25 ± 3.57%, respectively) at a dose of 100 μg/mL (Figures 5B and C). MCP-1 also significantly inhibited IL-6 production (30.51 ± 3.25%) at a dose of 50 μg/mL (Figure 5D). These results suggest that MCP-1 may act as a potential anti-inflammatory agent.

Network pharmacology based research into the effect against inflammation

A total of 192 potential targets of MCP-1 were identified (Figure 6A), and 330 inflammation-related targets were retrieved from the GeneCards database and 174 from the DisGeNET database. As shown in Figure 6B, 9 common targets were identified through a Venn diagram, including TLR4, STAT3, MMP9, COL18A1, TLR9, ABCB1, PPARA, MMP2, and NR1H4.

The PPI network of MCP-1 was constructed by importing core target data from STRING (combined score > 0.4) into Cytoscape software (Figures 6C and D). Key target proteins such as STAT3, MMP9, MMP2, and TLR4 were identified as central to the network, suggesting their significant role in the management of inflammation.

GO functional and KEGG pathway enrichment analysis

The results of the GO functional analysis are presented in Figure 7A, which includes 21 terms: 11 related to BP ($p<0.001$), 5 to CC ($p<0.05$), and 5 to MF ($p<0.01$). The BP terms included positive regulation of transcription from the RNA polymerase II promoter (GO:0045944), cellular response to LPS (GO:0071222), intracellular receptor signaling pathway (GO:0030522), positive regulation of interleukin-10 production (GO:0032733), positive regulation of cell migration (GO:0030335), positive regulation of interleukin-8 production (GO:0032757), negative regulation of IL-6 production (GO:0032715), inflammatory response (GO:0006954), positive regulation of IL-6 production (GO:0032755), and positive regulation of TNF-α production (GO:0032760), as well as positive regulation of gene expression (GO:0010628). In the

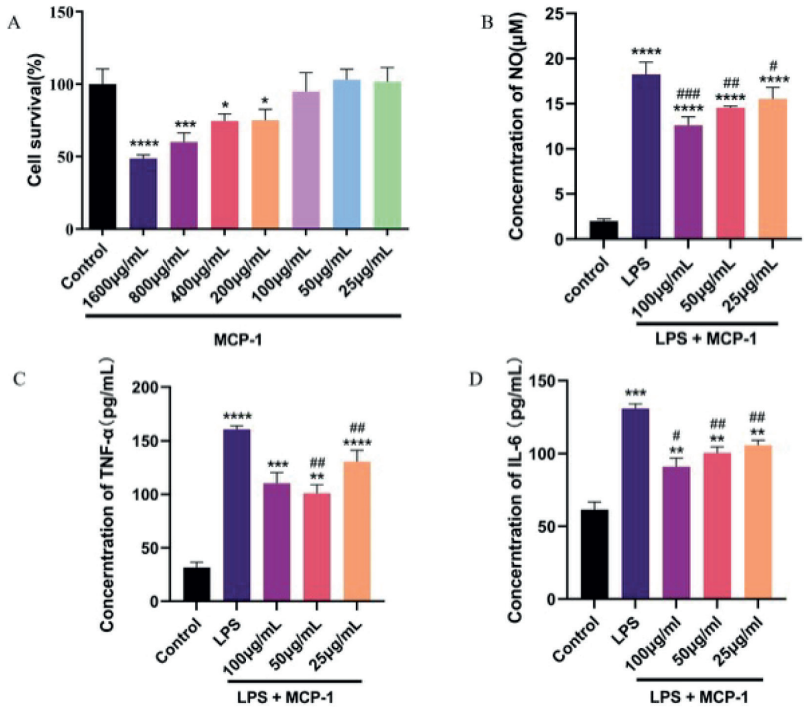

FIGURE 5 - Anti-inflammatory experiments of MCP-1.Toxicity of different concentrations of MCP-1 on RAW264.7 cells(A); Effect of MCP-1 on NO secretion by RAW264.7 cells induced by LPS (B); Effect of MCP-1 on TNF-α secretion by RAW264.7 cells after induction of LPS (C);Effect of MCP-1 on IL-6 secretion by RAW264.7 cells after LPS-induced(D). #p<0.05, ##p<0.01, ###p<0.001 compared with control group, *p<0.05, **p<0.01, ***p<0.001, ****p<0.0001 compared with LPS treatment group.

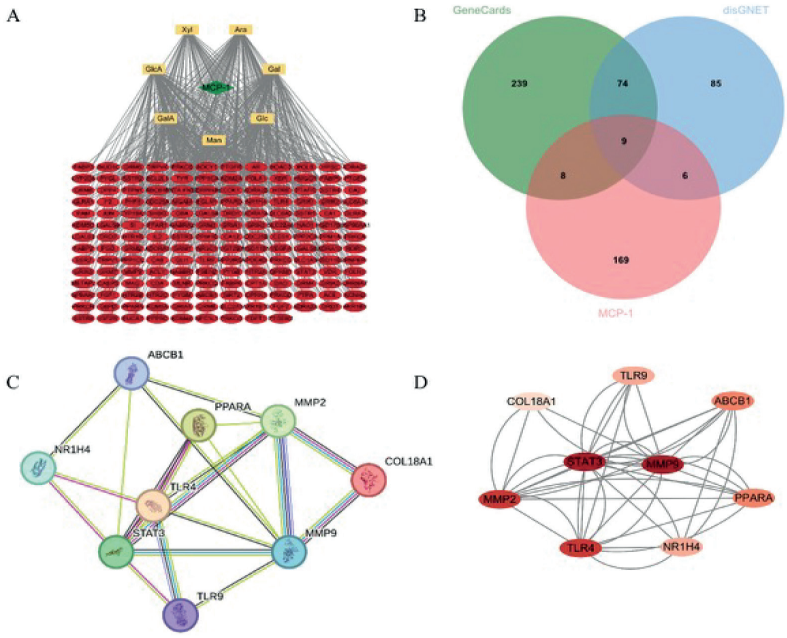

FIGURE 6 - PPI Analysis of Targets of MCP-1 against inflammation. Components-targets-network of MPC-1(A); Venn diagram of targets from inflammation and MCP-1(B); PPI network of potential targets of MCP-1 in the treatment of inflammation (C); PPI network of targets (D).

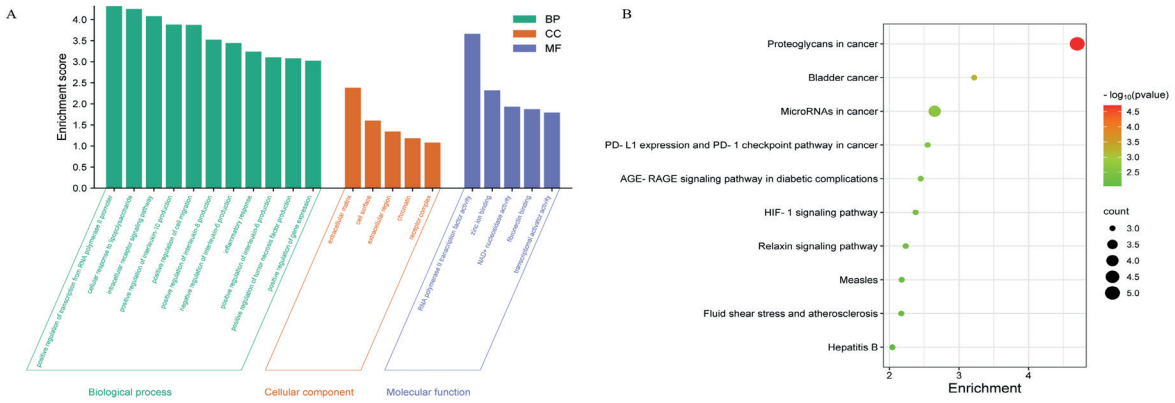

FIGURE 7 - Bioinformatics analysis of target proteins of MCP-1 against inflammation. GO function enrichment of targets from MCP-1 against inflammation (A); KEGG enrichment of targets from MCP-1 against inflammation(B).

CC category, significant terms included extracellular matrix (GO:0031012), cell surface (GO:0009986), extracellular region (GO:0005576), chromatin (GO:0000785), and receptor complex (GO:0043235). The MF terms included RNA polymerase II transcription factor activity, ligand-activated sequence-specific DNA binding (GO:0004879), zinc ion binding (GO:0008270), NAD+ nucleosidase activity (GO:0003953), fibronectin binding (GO:0001968), transcriptional activator activity, and RNA polymerase II transcription regulatory region sequence-specific binding (GO:0001228). In Figure 7B, the KEGG involved pathways ($p<0.01$) were mainly the Proteoglycans in cancer (hsa05205), Bladder cancer (hsa05219), MicroRNAs in cancer (hsa05206), PD-L1 expression and PD-1 checkpoint pathway in cancer (hsa05235), AGE-RAGE signaling pathway in diabetic complications (hsa04933), HIF-1 signaling pathway (hsa04066), Relaxing signaling pathway (hsa04926), Measles (hsa05162), Fluid shear stress and atherosclerosis (hsa05418), and Hepatitis B (hsa05161).

Molecular docking

Molecular docking was performed between 7 monosaccharides in MCP-1 and 9 key targets using AutoDock Vina software. Figure 8 shows that all seven monosaccharides could bind to the nine key targets. GalA, Glc, Ara, and Man exhibited the lowest binding energies to MMP2. Xyl demonstrated the lowest binding energy to PPARA. GlcA showed the lowest binding energy to STAT3, whereas Gal exhibited the lowest binding energy to MMP9. The residues involved are listed in Table I.

The binding energy (-6.686 kcal/mol) of GalA-MMP2 was the lowest. Figures 9 and 10 present the 2D and 3D interaction diagrams of GalA-MMP2, showing that GalA formed hydrogen bonds with the residues His121, Ala140, Leu117, Thr144, Pro135, His142, Leu138, and Ala137. Ara (18.31%), GalA (13.98%), and Glc (39.05%) were the three monosaccharides with the highest content in MCP-1 (Table I), and all exhibited the lowest binding energies to MMP2. This suggests that MMP2 may be a potential target of MCP-1 for treating inflammation.

DISSCUSION

Chinese herbal medicine polysaccharides have been shown to improve immune function, enhancing humoral, cellular, and mucosal immunity, and promoting overall immune health (Wan *et al.*, 2022). Polysaccharides

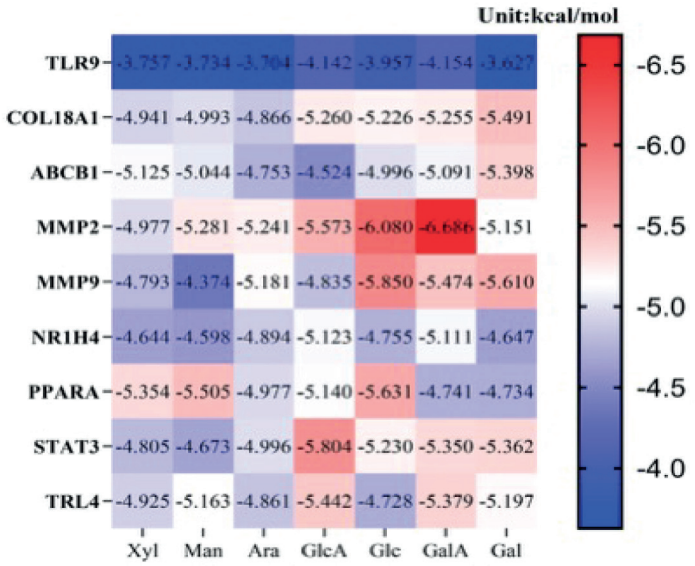

FIGURE 8 - Binding energy of 7 monosaccharide components to 9 target proteins.

TABLE I - The residues formed hydrogen bonds of each monosaccharides to targets with the lowest binding energy

Moleclues name	Content in MCP-1	Targets	Hydrogen bonds with residues
Glc	39.05%	MMP2	Leu117, Ala140, His121, Leu138, Ile142, Ala137, Pro135 and Thr144
Ara	18.31%	MMP2	Ala140, Ile142, Pro141, Asp3 and Ala84
Gal	14.80%	MMP9	Ala189, Leu188, Glu402 and Tyr420
GalA	13.98%	MMP2	His121, Ala140, Leu117, Thr144, Pro135, He142, Leu138 and Ala137
Xyl	7.42%	PPARA	Met220, Glu286, Thr283 and Thr279
Man	4.14%	MMP2	Asp3, Ala84, Pro141 and Leu83
GlcA	2.30%	STAT3	Ser540, Asn538, Tyr539, Val537, Thr526, Ile522 and Asp502

from *M. chinensis* have also been reported to repair liver damage (Hong *et al.*, 2023). Furthermore, studies have demonstrated the immunomodulatory effects of *M. chinensis* polysaccharides (Shen *et al.*, 2021). However, polysaccharides extracted through water and alcohol precipitation are not pure, often containing impurities such as pigments and lipids (Seedevi *et al.*, 2018). Thus, chromatography columns are necessary for further purification, isolating polysaccharides within a specific molecular weight range to obtain a homogeneous preparation. DEAE-52, a cellulose column packing, effectively adsorbs impurities like

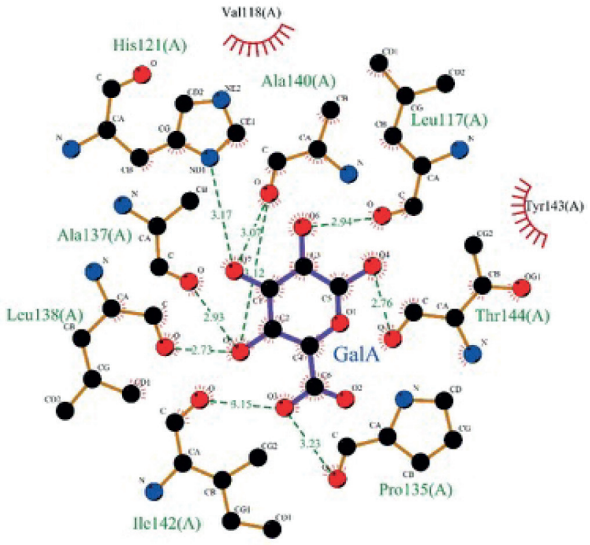

FIGURE 9 - The 2D interaction diagrams of GalA-MMP2.

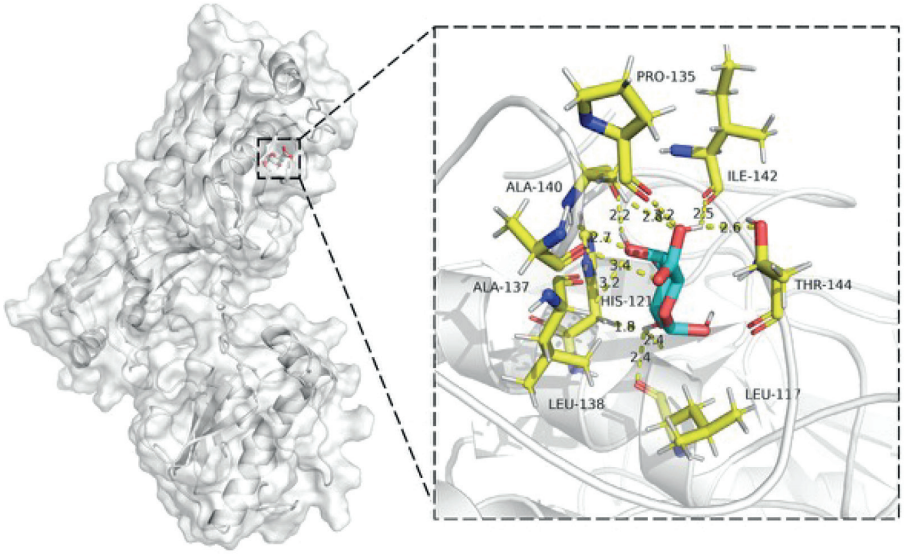

FIGURE 10 - The 3D interaction diagrams of GalA-MMP2.

pigments and lipids. Polysaccharides were attached to the DEAE-52 column and eluted with NaCl solutions at concentrations of 0.05 M, 0.10 M, and 0.15 M to collect different fractions. In subsequent freeze-drying, only the 0.05 M fraction could be redissolved, and thus this fraction was selected for further analysis. Sephadex G-100, a gel filtration medium, effectively isolates polysaccharides with molecular weights between 4,000 and 150,000 (Udchumpisai and Bangyeekhun, 2020). Polysaccharides with similar molecular weights were retained by Sephadex G-100, yielding a homogeneous polysaccharide (MCP-1) with a molecular weight of 70.9kDa Our analysis indicated that MCP-1 has a triple helix configuration, featuring common functional groups such as C-O, C=O, -OH, and β-glycosidic bonds. SEM and AFM were employed to analyze the

structure of MCP-1, revealing a thick, flaky appearance with substantial pieces and particles, corresponding to heights of 327.3 nm and 389.8 nm, respectively. The homogeneous polysaccharide MCP-1 consists of glucose (39.05%), arabinose (18.31%), galactose (14.80%), galacturonic acid (13.98%), xylose (7.42%), mannose (4.14%), and glucuronic acid (2.30%). Some of these monosaccharides are known to possess anti-inflammatory properties. Mannose has been shown to induce regulatory T cells whereas inhibiting effector T cells and inflammatory macrophages, thereby reducing inflammation (Zhang *et al.*, 2021). Arabinose has demonstrated the ability to inhibit colitis by downregulating pro-inflammatory genes in CaCO-2 cells (Li *et al.*, 2019). Polysaccharides from *Ginkgo biloba*, rich in galacturonic acid and galactose, have also been confirmed to have anti-inflammatory effects (Li *et al.*, 2022). Based on this, we aimed to investigate the anti-inflammatory activity of MCP-1.

Inflammation involves processes such as tissue injury, immune system activation, and the secretion of inflammatory mediators (Chen *et al.*, 2018). The inhibition of nitric oxide (NO), TNF-α, and IL-6 production in LPS-induced RAW264.7 cells is a standard method for evaluating anti-inflammatory activity (Lima *et al.*, 2021). Previous studies have shown that MCP-1 can significantly inhibit the production of NO, IL-6, and TNF-α (30.79 ± 4.13%, 30.51 ± 3.25%, and 37.25 ± 3.57%, respectively), suggesting its potential as an anti-inflammatory agent. However, the underlying mechanisms by which MCP-1 interacts with anti-inflammatory targets remain unclear. This is a common issue with Chinese herbal polysaccharides: strong efficacy without a clear mechanism. Network pharmacology techniques can be used to establish a compounds-targets-pathways network, enabling the identification of potential anti-inflammatory targets in polysaccharides. In this study, 169 potential disease targets were identified for MCP-1, and 9 inflammation-related targets were selected: TLR4, STAT3, MMP9, COL18A1, TLR9, ABCB1, PPARA, MMP2, and NR1H4. These targets were used to construct a protein-protein interaction (PPI) network, and GO and Kyoto Encyclopedia of Genes and Genomes (KEGG) enrichment analyses were performed.

The PPI network analysis identified STAT3, MMP9, MMP2, and TLR4 as key targets. GO functional analysis revealed that inflammation-related BP were primarily associated with the positive regulation of interleukin-10 (IL-10) production, negative regulation of IL-6 production, positive regulation of TNF-α production, and positive regulation of RNA polymerase II transcription. Inflammation is the host immune response initiated by tissues to combat danger signals during infection or injury. IL-6, a complex multifunctional cytokine, plays a key role in promoting hematopoiesis, regulating the acute-phase response, and initiating immune responses. Elevated IL-6 levels are considered an effective indicator of inflammation (Nishimoto *et al.*, 1999). Chronic inflammation is often directly associated with elevated levels of TNF-α in the body. Improper or excessive activation of the TNF-α signaling pathway can lead to various inflammatory diseases, including autoimmune disorders (Jang *et al.*, 2021). The ability of IL-10 to suppress the production of TNF-α and IL-6 induced by LPS was significantly diminished in both alveolar and peritoneal macrophages from infected murine models. The reactivity of IL-10 was not directly related to receptor expression; however, exposure of normal macrophages to high concentrations of TNF-α markedly reduced their responsiveness to IL-10 (Avdiushko *et al.*, 2001). RNA polymerase II, an enzyme present in eukaryotic cells, is involved in transcription. Identifying RNA polymerase II within extensive sequences could uncover new transcriptional sites and improve our understanding of the mechanisms regulating transcriptional elongation (Brodsky *et al.*, 2005). KEGG pathway analysis suggested that MCP-1 could modulate inflammation through various pathways, including PD-L1, PD-1, and HIF-1. In summary, it is hypothesized that the anti-inflammatory activity of MCP-1 may be mediated by promoting IL-10 secretion.

Molecular docking studies were conducted to evaluate the binding interactions between the 9 disease-

related targets and the 7 monosaccharide components of MCP-1, with the aim of identifying potential anti-inflammatory targets. The results indicated that the monosaccharides GalA, Glc, Ara and Man showed the lowest binding energies with MMP2. Among them, GalA exhibited the strongest binding affinity with MMP2, with a docking energy of -6.686 kcal/mol. Matrix metalloproteinases (MMPs), particularly MMP2, are associated with inflammatory conditions such as osteoarthritis and rheumatoid arthritis (Milaras *et al.*, 2021). MMP2 is involved in tumor progression and bone tissue development, and its overactivation can contribute to osteolytic destruction, leading to inflammation (Li *et al.*, 2021). Thus, we hypothesize that MCP-1 alleviates inflammation by reducing osteolytic destruction through the inhibition of MMP2.

CONCLUSION

This manuscript reports the isolation of a homogeneous polysaccharide from *M. chinensis*, designated as MCP-1. The polysaccharide was characterized by a triple helix structure and was predominantly composed of glucose (39.05%), arabinose (18.31%), galactose (14.80%), galacturonic acid (13.98%), xylose (7.42%), mannose (4.14%), and glucuronic acid (2.30%). The molecular weight of MCP-1, as measured by GPC, was 70.9kDa, with the measured heights of the particles and pieces recorded at 327.3 nm and 389.8 nm, respectively. Furthermore, the results indicated that MCP-1 exhibited significant anti-inflammatory activity, as evidenced by a decrease in the release of NO, TNF-α, and IL-6 (30.79±4.13%, 37.25±3.57%, and 30.51±3.25%, respectively). A total of 169 targets were identified based on the monosaccharide structures of MCP-1, with 9 of these targets associated with inflammation, including TLR4, STAT3, MMP9, COL18A1, TLR9, ABCB1, PPARA, MMP2, and NR1H4. The principal targets for anti-inflammatory activity were found to be associated with several signaling pathways, including those related to cancer and immune responses. Molecular docking results demonstrated that MCP-1 exhibited a high binding affinity to MMP2. Based on these findings, it can be reasonably proposed that MCP-1 represents a promising candidate for addressing inflammation in both the food and pharmaceutical industries.

ACKNOWLEDGMENTS

This study received financial support from the National Natural Science Foundation of China (82073977), the General Project of Guangdong Natural Science Foundation (2023A1515011445), the Guangdong joint research fund with enterprises (2022A1515220142).

DATA AVAILABILITY STATEMENT

All data is available within the article or its supplementary materials.

REFERENCES

Avdiushko R, Hongo D, Lake-Bullock H, Kaplan A, Cohen D. IL-10 receptor dysfunction in macrophages during chronic inflammation. J Leukoc Biol. 2001;70(4):624-632.

Bradford MM. A rapid and sensitive method for the quantitation of microgram quantities of protein utilizing the principle of protein-dye binding. Anal Biochem. 1976;72:248-254.

Brodsky AS, Meyer CA, Swinburne IA, Hall G, Keenan BJ, Liu XS, et al. Genomic mapping of RNA polymerase II reveals sites of co-transcriptional regulation in human cells. Genome Biol. 2005;6(8):R64.

Chen L, Deng H, Cui H, Fang J, Zuo Z, Deng J, et al. Inflammatory responses and inflammation-associated diseases in organs. Oncotarget. 2018;9(6):7204-7218.

DuBois M, Gilles KA, Hamilton JK, Rebers PA, Smith F. Colorimetric Method for Determination of Sugars and

Related Substances. Anal Chem. 1956;28(3):350-356.

Guo X, Kang J, Xu Z, Guo Q, Zhang L, Ning H, et al. Triple-helix polysaccharides: Formation mechanisms and analytical methods. Carbohydr Polym. 2021;262:117962.

Hoseiniyan Benvidi SM, Jahanbin K. A new water-soluble polysaccharide from Echinops pungens Trautv roots. Part I. Isolation, purification, characterization and antioxidant activity. Int J Biol Macromol. 2020;161:909-916.

Hou C, Chen L, Yang L, Ji X. An insight into anti-inflammatory effects of natural polysaccharides. Int J Biol Macromol. 2020;153:248-255.

Hong Y, Shen M, Yu Q, Chen Y, Xie J. UPLC-Q-TOF/MS-based metabolomics reveals modulatory effects of Mesona chinensis Benth polysaccharide in liver injury mice induced by cyclophosphamide. Food Sci Human Wellness. 2023;12(2):584-595.

Huang J, Ding L, Tian W, Zhi H, Chen J, Wu L, et al. Polyphaenolic profiling, antioxidant properties, and inhibition of α-glucosidase of Mesona chinensis benth from Southern China. Microchem J. 2021;168:106399.

Jang DI, Lee AH, Shin HY, Song HR, Park JH, Kang TB, et al. The Role of Tumor Necrosis Factor Alpha (TNF-α) in Autoimmune Disease and Current TNF-α Inhibitors in Therapeutics. Int J Mol Sci. 2021;22(5):2719.

Li X, Jin L, Tan Y. Different roles of matrix metalloproteinase 2 in osteolysis of skeletal dysplasia and bone metastasis (Review). Mol Med Rep. 2021;23(1):70-76.

Li X, Wang Z, Wang L, Walid E, Zhang H. Ultrasonic-assisted extraction of polysaccharides from Hohenbuehelia serotina by response surface methodology. Int J Biol Macromol. 2012;51(4):523-530.

Li Y, Pan H, Liu J-x, Li T, Liu S, Shi W, et al. l-Arabinose Inhibits Colitis by Modulating Gut Microbiota in Mice. J. Agric. Food Chem. 2019;67(48):13299-13306.

Li Y, Sheng Y, Liu J, Xu G, Yu W, Cui Q, et al. Hair-growth promoting effect and anti-inflammatory mechanism of Ginkgo biloba polysaccharides. Carbohydr Polym. 2022;278:118811.

Mandelli L, Milaneschi Y, Hiles S, Serretti A, Penninx BW. Unhealthy lifestyle impacts on biological systems involved in stress response: hypothalamic-pituitary-adrenal axis, inflammation and autonomous nervous system. Int Clin Psychopharmacol. 2023;38(3):127-135.

Milaras C, Lepetsos P, Dafou D, Potoupnis M, Tsiridis E. Association of Matrix Metalloproteinase (MMP) Gene Polymorphisms With Knee Osteoarthritis: A Review of the Literature. Cureus. 2021;13(10):e18607.

Nishimoto N, Kishimoto T, Yoshizaki K. Anticytokine therapy in autoimmune diseases. Intern Med. 1999;38(2):178-182.

Seedevi P, Moovendhan M, Sudharsan S, Sivasankar P, Sivakumar L, Vairamani S, et al. Isolation and chemical characteristics of rhamnose enriched polysaccharide from Grateloupia lithophila. Carbohydr Polym. 2018;195:486-494.

Shen M, Chen X, Huang L, Yu Q, Chen Y, Xie J. Sulfated Mesona chinensis Benth polysaccharide enhance the immunomodulatory activities of cyclophosphamide-treated mice. J Funct Food. 2021;76:104321.

Sun M, Li Y, Wang T, Sun Y, Xu X, Zhang Z. Isolation, fine structure and morphology studies of galactomannan from endosperm of Gleditsia japonica var. delavayi. Carbohydr Polym. 2018;184:127-134.

Udchumpisai W, Bangyeekhun E. Purification, Structural Characterization, and Biological Activity of Polysaccharides from Lentinus velutinus. Mycobiology. 2020; 48(1):51-57.

Wan X, Yin Y, Zhou C, Hou L, Cui Q, Zhang X, et al. Polysaccharides derived from Chinese medicinal herbs: A promising choice of vaccine adjuvants. Carbohydr Polym. 2022;276:118739.

Zhang W, Cheng H, Gui Y, Zhan Q, Li S, Qiao W, et al. Mannose Treatment: A Promising Novel Strategy to Suppress Inflammation. Front Immunol. 2021;12:756920.

Zhang P, Tan J, Wang W, Zhang J, Gong H, Xue H. Extraction, Separation, Purification, Chemical Characterizations, and Biological Activities of Polysaccharides from Chinese Herbal Medicine: A Review. Starch-Starke. 2022;74(11-12):2200114.

Zhao Y, Yan B, Wang Z, Li M, Zhao W. Natural Polysaccharides with Immunomodulatory Activities. Mini Rev Med Chem. 2020;20(2):96-106.

Zhao L, Zhang H, Li N, Chen J, Xu H, Wang Y, et al. Network pharmacology, a promising approach to reveal the pharmacology mechanism of Chinese medicine formula. J Ethnopharmacol. 2023;309:116306.

Zheng Y, Bai L, Zhou Y, Tong R, Zeng M, Li X, et al. Polysaccharides from Chinese herbal medicine for anti-diabetes recent advances. Int J Biol Macromol. 2019;121:1240-1253.

Received for publication on April 12th, 2024
Accepted for publication on July 4th, 2024
Associated Editor: Taís Gratieri